

# Thermophysical properties of phase change emulsions prepared by D-phase emulsification



Takashi Morimoto<sup>a,\*</sup>, Kenichi Togashi<sup>a</sup>, Hiroyuki Kumano<sup>a</sup>, Hiki Hong<sup>b</sup>

<sup>a</sup> Department of Mechanical Engineering, Aoyama Gakuin Univ., 5-10-1, Fuchinobe, Chuo-ku, Sagami-hara 252-5258, Japan

<sup>b</sup> Department of Mechanical and Industrial System Engineering, Kyung Hee Univ., 449-701 Yong-in, Kyung-gi, South Korea

## ARTICLE INFO

### Article history:

Received 1 February 2016

Received in revised form 13 May 2016

Accepted 22 May 2016

### Keywords:

PCE

PCM

Phase change

Viscosity

Latent heat

## ABSTRACT

A phase change emulsion (PCE) is a mixture of fine particles of a phase change material (PCM) and an aqueous surfactant solution. PCEs are attracting attention as thermal media. They provide high-density thermal energy storage by utilizing the latent heat of the PCM, and high transportability because of their high fluidity. In this study, PCEs were prepared by D-phase emulsification, and their properties were evaluated. Two paraffin PCMs, n-hexadecane and n-octadecane, were dispersed inside the PCEs, and their mass fraction was varied. The PCEs exhibited similar particle size distributions, regardless of the type of dispersed PCM or its mass fraction. The viscosity of the PCE increased with increasing PCM mass fraction, in agreement with theoretical values. The latent heat of fusion and specific heat of the PCEs were evaluated using a temperature history method. Pump consumption rates were calculated from these results, and are compared with that of water.

© 2016 Elsevier Ltd. All rights reserved.

## 1. Introduction

In recent years, thermal energy storage techniques have been developed to utilize thermal energy efficiently. The latent heat storage system is one of thermal energy storage techniques. Phase change materials (PCMs) are a type of heat storage material, and can be used as a thermal medium in such systems [1–5]. Desirable properties in a thermal medium are: (a) a melting point within a temperature range suited to a given purpose; (b) a large latent heat per volume; (c) reliable and stable operation during solidifying-melting cycles; (d) good temperature response; and (e) small volume change during phase change. Phase change slurries (PCSs) are recognized as thermal media that satisfy these conditions to some extent. Thermal energy is easily transported at low cost using PCSs, because they can be readily pumped. Thermal energy can also be released more quickly, because of their convective heat transfer [6–8]. However, practical PCSs are often face problems including tube obstruction induced by PCM sedimentation, irregular flow resulting from their rheological characteristics, separation of PCM particles due to density difference between continuous phase and dispersed phase [9]. Furthermore, when they are stored in a tank, agitation is required for homogeneous dispersion and to avoid agglomeration of particles [10,11].

Phase change emulsions (PCEs) are an alternative to PCSs, which have the potential to overcome these problems [12–16]. PCEs consist of an aqueous solution and PCM particles which are homogeneously dispersed in it. PCM particles in PCEs keep stable dispersion under any conditions. Therefore, PCEs can be transported in channels of any shape and size maintaining a homogeneous flow without tube jam and required agitation in storage tank.

Inaba et al. [12] evaluated the thermophysical properties of a PCE with n-tetradecane particles. They prepared an emulsion using mechanical emulsification and its average diameter is 3.4  $\mu\text{m}$ . Chen et al. [13] reported that the pump consumption of a PCE system for a given heat transportation quantity was much lower than that of water, and it is attributed to phase change. They prepared emulsions using PIC method. The average diameter of the emulsion which containing 30 mass% n-tetradecane is 51.0  $\mu\text{m}$ .

PCEs with high dispersing stability are desired for stable operation of PCE systems. However, PCEs can break down (e.g. coalescing, creaming) if they are not prepared properly. The stability of a PCE depends on its particle size. Many methods are utilized to prepare emulsions with fine particles and one of them is D-phase emulsification [17]. Kumashiro et al. [18] prepared a PCE by D-phase emulsification. The emulsion shows a stable dispersion with high durability to cyclical temperature changes, so it seems to be a prospective thermal storage medium. However, detailed thermophysical properties of PCEs prepared by D-phase emulsification,

\* Corresponding author.

E-mail address: [c5615124@aoyama.jp](mailto:c5615124@aoyama.jp) (T. Morimoto).

## Nomenclature

$A$	heat transfer area [m <sup>2</sup> ]
$Bi$	Biot number [-]
$C$	crowding factor [-]
$c_p$	specific heat [kJ/(K kg)]
$D$	circular tube diameter [m]
$d_{ave}$	average diameter [ $\mu$ m]
$\Delta h_{ls}$	latent heat [kJ/kg]
$I$	integrated value [K s]
$k$	thermal conductivity [W/(m K)]
$L$	circular tube length [m]
$m$	mass [kg]
$P$	pumping power [W]
$R$	outer radius of test tube [m]
$Re$	Reynolds number [-]
$T$	temperature [K]
$t$	time [s]
$u$	flow velocity [m/s]

### Greek symbols

$\alpha$	heat transfer coefficient [W/(m <sup>2</sup> K)]
$\phi$	volume fraction [vol.%]
$\eta_{rel}$	relative viscosity [-]

$\eta_{lim}$	limit viscosity [-]
$\mu$	viscosity [Pa s]
$\rho$	density [kg/m <sup>3</sup> ]

### Subscripts

alc	alcohol
con	continuous phase
e	environment
i	inflection point
l	liquid
m	melting point
M	Mooney's equation
O	initial
PCM	phase change material
PCE	phase change emulsion
s	solid
surf	surfactant
t	test tube
T	Thomas' equation
w	water

and their dependence on the PCM mass fraction have not yet been clarified.

In the present study, the particle size distribution, viscosity, rheological behavior, specific heat, and latent heat of solidification of PCEs were evaluated experimentally. Two paraffin PCMs, n-hexadecane (melting point: 18.2 °C) and n-octadecane (melting point: 28.2 °C) were used as the dispersed phases of PCEs, and their mass fractions were varied.

## 2. D-phase emulsification

### 2.1. Procedure

D-phase emulsification was carried out as follows. An alcohol, water and surfactant were mixed in a certain ratio, yielding a mixture called the D-phase. Liquid oil was added to the D-phase, and the mixture was stirred until an oil-in-D-phase (O/D) gel emulsion is formed. Here, "liquid oil" means not only PCMs but also other oils (e.g. silicone oil, sesame oil) and they can be dispersed using D-phase emulsification. The O/D gel emulsion was then diluted with water, and the mixture was stirred, forming an oil-in-water (O/W) emulsion. In this study, 1,3-butandiol was used as the alcohol, polyoxyethylene (20) sorbitan monooleate (HLB value = 15) as the surfactant, and n-hexadecane and n-octadecane as the oil/PCM. The properties of the PCMs and water are shown in Table 1. A detailed emulsification procedure is given below. At first, 2.0 g of water, 2.0 g of alcohol, and 4.0 g of surfactant are mixed and D-phase is yielded from the mixture. Next, 10.0 g of liquid PCM was slowly added to the above D-phase, and stirred until the O/D gel

is formed (water: alcohol: surfactant: PCM mass ratio = 1:1:2:5). Finally, the gel was diluted by adding 82.0 g of water and then an 100.0 g of O/W type PCE which contains 10.0 mass% of PCM is generated. The PCM content was changed by adjusting the amount of dilution water, yielding PCEs containing 10.0, 16.7, 20.0, 25.0, 30.0, and 40.0 mass% of PCM.

As mentioned above, stable emulsions with fine particles can be generated by D-phase emulsification. Reducing interfacial tension is important to generate emulsions with small particles. However, if the interfacial tension is reduced too much, the particles coalesce easily. Using D-phase emulsification, the interfacial tension is kept properly, because O/D gel emulsion at the 2nd stage of D-phase emulsification is generated with proper interfacial tension. Moreover, the method does not require precise adjustment of the HLB value, which is important property of surfactants. Generally, it is regarded that HLB value range required to generate stable emulsion is 8.2–12.9. On the other hand, using D-phase emulsification, the range is expanded to 8.2–15.3. HLB value of the surfactant which is used in the present study is 15. If other emulsifications are used, adjustment of HLB value is required but it isn't required for D-phase emulsification.

### 2.2. Particle size distribution

The particle size distributions of the PCMs were measured using a laser diffraction particle size analyzer (HORIBA, NANO PARTICLE ANALYZER SZ-100). Fig. 1 shows the particle size distributions of PCEs with PCM mass fractions of 10.0–40.0 mass%. n-Hexadecane or n-octadecane was dispersed as the PCM. Similar distributions

**Table 1**  
Thermophysical properties of the PCMs and water.[19]

	Melting point [°C]	Latent heat of fusion [kJ/kg]	Heat conductivity [W/(m K)] Solid (liquid)	Density [kg/m <sup>3</sup> ] Solid (liquid)	Specific heat [kJ/(kg K)] Solid (liquid)
n-Hexadecane	18.2	229	0.34 (0.15)	830 (780)	1.8 (2.2)
n-Octadecane	28.2	243	0.34 (0.15)	830 (780)	1.8 (2.2)
Pure water	0	334	(0.61)	(997)	4.18

were observed for the three PCEs, despite their different PCM type and mass fractions. The average particle size of the 10.0 mass% n-hexadecane PCE was 223 nm, the 20.0 mass% n-octadecane PCE was 222 nm, and the 40.0 mass% n-octadecane PCE was 246 nm. Generally, average particle size of PCEs which are prepared by other emulsifications (e.g. mechanical emulsification, PIC method) is around 1–100  $\mu\text{m}$  (i.e., [12,13]). The similarity in particle size distributions is attributed to the D-phase emulsification process. The procedure and amount of reagent added to form the O/D gel were constant for all the emulsions prepared in the present study, and the PCM mass fraction was controlled by just adjusting the amount of dilution water. The particle sizes were therefore likely to be determined when the PCM was dispersed in the D-phase.

### 3. Evaluation of physical properties

#### 3.1. Rheological behavior of PCEs

The rheological behavior of the PCEs were evaluated by a rheometer (Brookfield, R/S-CC plus). Fig. 2 shows the relationship between the shear rate and shear stress of the PCEs at 25.0  $^{\circ}\text{C}$ . PCEs containing 10.0–30.0 mass% of PCM were considered Newtonian fluids, because the relationship between their shear rate and shear stress was almost linear. The PCE containing 40.0 mass% of PCM was considered a pseudoplastic fluid at low shear rate [0–500 (1/s)]. However, the relationship between its shear rate and shear stress became more linear at high shear rates. Inside the PCEs with high volume fraction of particles, it is possible that the PCM particles formed an invertible aggregation structures because of the increased volume fraction of PCM and the structure are conserved during the measurement in the low shear rate range. On the other hand, in the high shear stress range, the aggregation structures are likely to be decomposed due to higher shear stress. Based on the mechanism mentioned above, the increase of the linearity in the high shear rate range might be attributed to the decomposition of the aggregation structure. Moreover, shear stress for two kinds of PCEs different, even though their particle size distribution is almost the same and the mass fraction of PCM is the same. However, the detailed mechanism is still unclear.

#### 3.2. Viscosity of PCEs

Fig. 3 shows the relationship between the PCM volume fraction ( $\phi$ ) and viscosity of PCE ( $\mu_{\text{PCE}}$ ) and viscosity of continuous phase ( $\mu_{\text{con}}$ ) at 25.0  $^{\circ}\text{C}$ . After the viscosities of the PCEs were measured, that of their continuous phases were also measured to calculate relative viscosity ( $\eta_{\text{rel}}$ ), which is defined by Eq. (1). A centrifuge was used to separate the continuous phases of the PCEs, to enable measurement of the continuous phase alone. Fulfilment of separation was judged by confirming that the PCE was divided into a milky-white particle-rich layer and a transparent continuous phase. After the continuous phase is separated, it was sampled and its viscosity was measured using the rheometer.

$$\eta_{\text{rel}} = \frac{\mu_{\text{PCE}}}{\mu_{\text{con}}} \quad (1)$$

The viscosity of the PCE increased with increasing PCM mass fraction, similar to general suspensions. Fig. 4 shows the relationship between PCM volume fraction and  $\eta_{\text{rel}}$ . Thomas' equation [20] and Mooney's equation [21] are the general viscosity prediction formulae for suspensions, and are given in Eqs. (2) and (3), respectively. Values of  $\eta_{\text{rel}}$  calculated using these two equations are compared with experimentally measured values in Fig. 4. Values of  $\eta_{\text{rel}}$  calculated using the viscosity of water as the continuous phase are also shown Fig. 5.

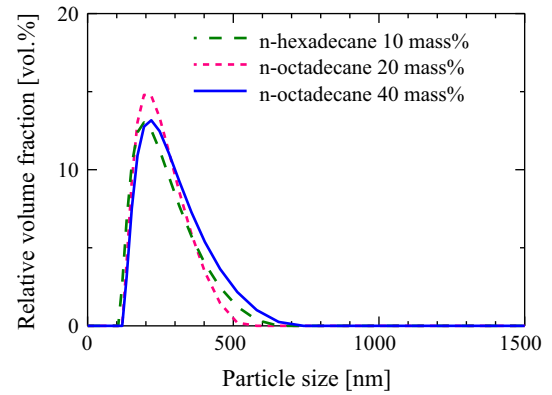
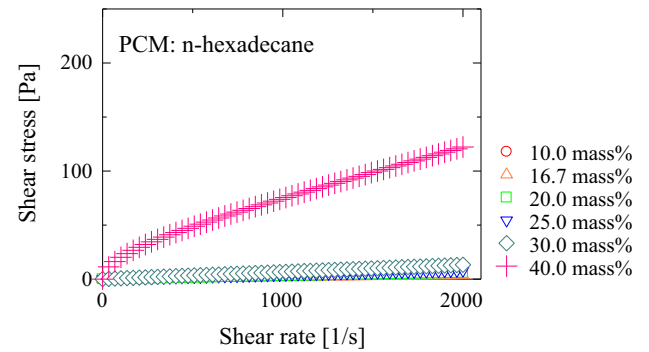
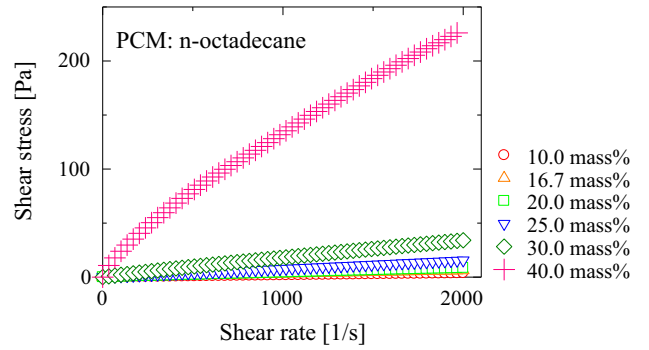


Fig. 1. Particle size distribution of PCEs.



(a) PCM: n-hexadecane



(b) PCM: n-octadecane

Fig. 2. Relations between shear stress and shear rate.

$$\eta_{\text{rel,T}} = \frac{\mu_{\text{PCE}}}{\mu_{\text{con}}} = \{1 + 2.5\phi + 10.05\phi^2 + 0.00273 \exp(16.6\phi)\} \quad (2)$$

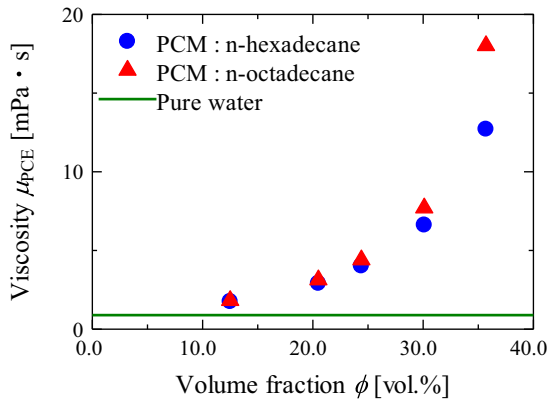
$$\eta_{\text{rel,M}} = \frac{\mu_{\text{PCE}}}{\mu_{\text{con}}} = \exp\left(\frac{\eta_{\text{lim}}\phi}{100 - C\phi}\right) \quad (3)$$

where  $\eta_{\text{lim}}$  is limit viscosity [22] and  $C$  is crowding factor. These are defined as following equations:

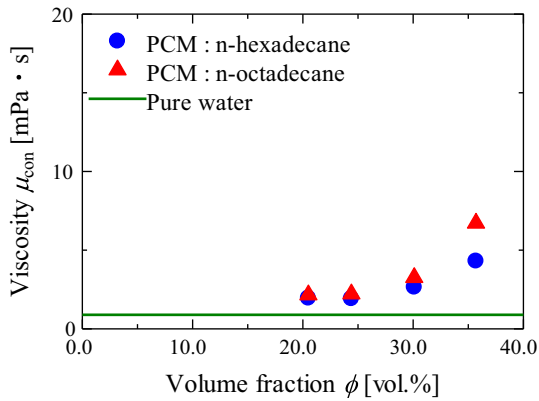
$$\eta_{\text{lim}} = \frac{\mu_{\text{con}} + 5\mu_{\text{PCM}}/2}{\mu_{\text{con}} + \mu_{\text{PCM}}} \quad (4)$$

$$C = \exp(0.096 + 0.0103d_{\text{ave}}^{-1} + 0.0290d_{\text{ave}}^{-2}) \quad (5)$$

In addition, the volume fraction of PCM ( $\phi$ ) was calculated from Eq. (6)



(a) Overall PCE



(b) Separated continuous phase

Fig. 3. Relations between viscosity and volume fraction.

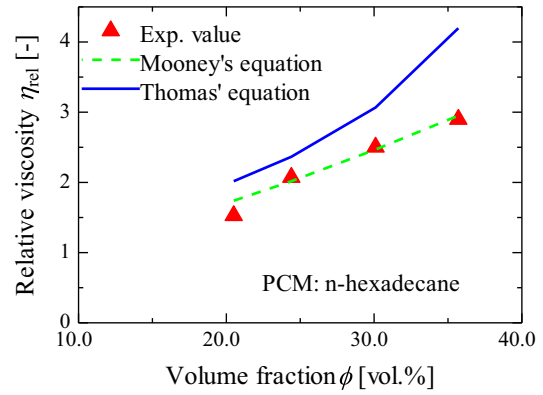
$$\phi = \frac{m_{\text{PCM}}/\rho_{\text{PCM}}}{m_{\text{surf}}/\rho_{\text{surf}} + m_{\text{alc}}/\rho_{\text{alc}} + m_{\text{w}}/\rho_{\text{w}} + m_{\text{PCM}}/\rho_{\text{PCM}}} \quad (6)$$

Fig. 4 shows that values of  $\eta_{\text{rel}}$  calculated from the experimental results agreed with Mooney's equation, when assuming the continuous phase is the surfactant aqueous solution. The experimental results didn't agree with Thomas' equation. This is because Thomas' equation is derived without considering effect of particle size and viscosity of continuous and dispersed phase. Fig. 5 shows that the results deviated significantly when considering the continuous phase as water. Therefore, the continuous phase viscosity of the PCEs should be used relative viscosity calculation. However, the PCE containing 35.0 vol.% n-octadecane showed a 10.8% deviation from Mooney's equation, despite its continuous phase was considered as a solution. In this study, the continuous phase was separated from the PCE by centrifugation, and complete separation was gauged visually. Thus, it is possible that separation was not complete, and that the separated continuous phase contained residual PCM particles. This would have resulted in the measured viscosity being higher than the true viscosity of the continuous phase, and the calculated relative viscosity therefore being lower. The other results agreed with Mooney's equation, so it was considered valid for the PCEs prepared by D-phase emulsification.

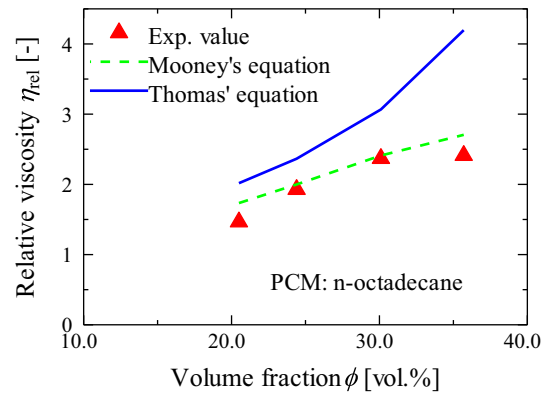
### 3.3. Evaluation of specific heat and latent heat

#### 3.3.1. Experimental apparatus and method

Temperature history (T-history) method [23] was used to measure the specific heat and latent heat. Thermophysical properties of objects can be measured from their temperature history, when the



(a) PCM: n-hexadecane



(b) PCM: n-octadecane

Fig. 4. Relationship between relative viscosity and volume fraction.  $\mu_{\text{con}}$  in Eqs. (2) and (3): measured viscosity of the separated continuous phase.

object and a reference material are located statically in an atmosphere and cooled or heated slowly. Fig. 6 shows a schematic of the experimental apparatus. The setup consisted of two test tubes suspended in a constant temperature room filled with air. The test tubes were surrounded by a container acting as a wind shield, to prevent forced-convective heat transfer on the surface of the test tubes. Five T-type thermocouples were installed, two of them to measure the bulk temperature of the material, and the others to measure the environmental temperature. Approximately 1.3 g of PCE and reference material (pure water) were filled to their respective test tubes. Their temperatures were set at a constant initial temperature ( $T_0$ ), which was above the melting point of the PCM suspending inside the PCE. The test tubes were then placed in the constant temperature room, and slowly cooled by natural convection of atmospheric air. Preliminary experiments were carried out to determine the environmental temperature ( $T_e$ ), because supercooling of PCM particles in PCEs has been widely reported [24], albeit in PCEs prepared by alternative methods from the present study. The melting points of n-hexadecane and n-octadecane are 18.2 and 28.2 °C, respectively, but solidification of the PCM particles did not occur upon cooling to about 2.4 and 13.7 °C, respectively. These temperatures were approximately 14.0 °C lower than the melting point of the each PCM. Therefore, the environmental temperature was set below the temperature at which the PCMs froze; −4.0 °C for the n-hexadecane PCE and 6.0 °C for the n-octadecane PCE.

The example of T-history data is shown in Fig. 7. The T-history of water decreased continuously, but the T-history of PCE showed a horizontal line because of latent heat release of PCM particles. The

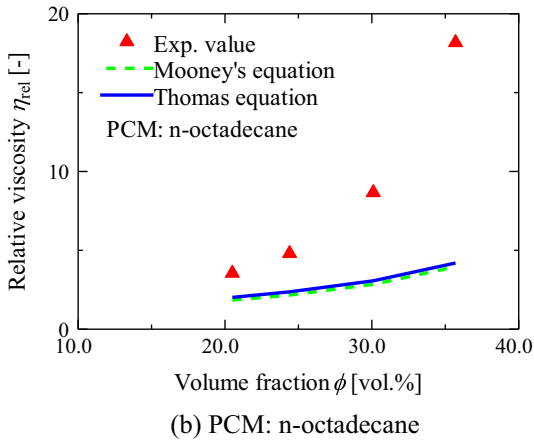
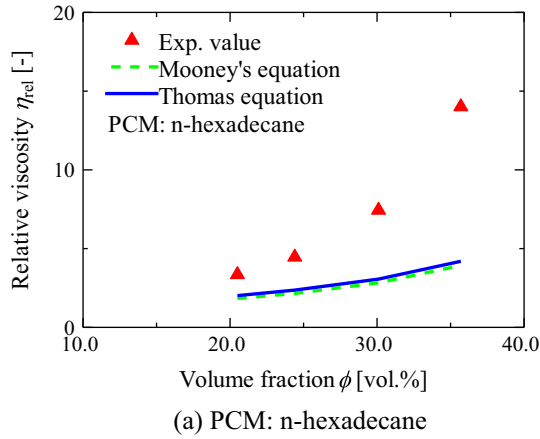


Fig. 5. Relationship between relative viscosity and volume fraction.  $\mu_{con}$  in Eqs. (2) and (3): A literature viscosity for pure water.

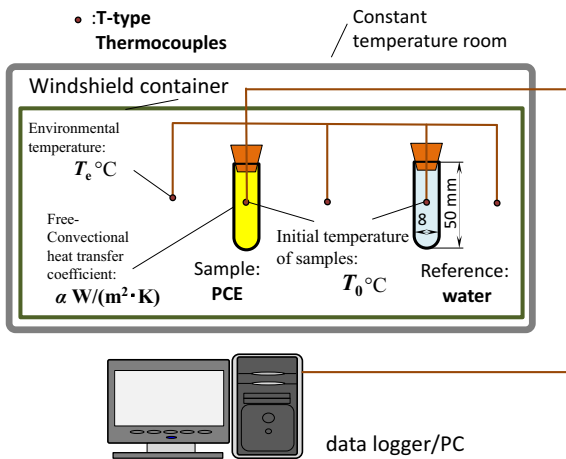


Fig. 6. Experimental apparatus for measuring specific heat and latent heat.

T-histories of each sample were divided into three periods; the liquid period, the phase change period and the solid period, as shown in Fig. 8. Assuming that solidification of the PCM proceeds during the phase change period (the range between the solidification starting point and inflection point in Fig. 8), then the specific heat during the liquid period, latent heat of solidification, and specific heat during the solid period can be calculated using Eqs. (7)–(9), respectively. The inflection point was determined as the point of maximum gradient on the T-history.

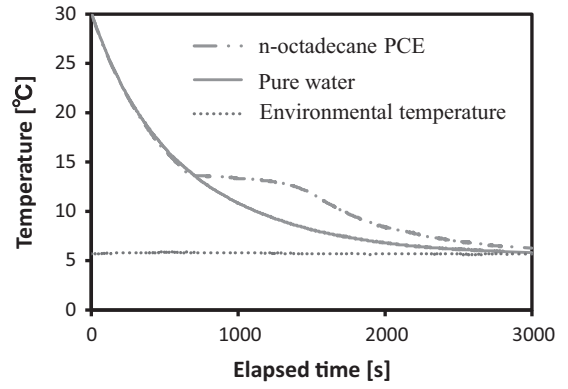


Fig. 7. Examples of temperature histories.

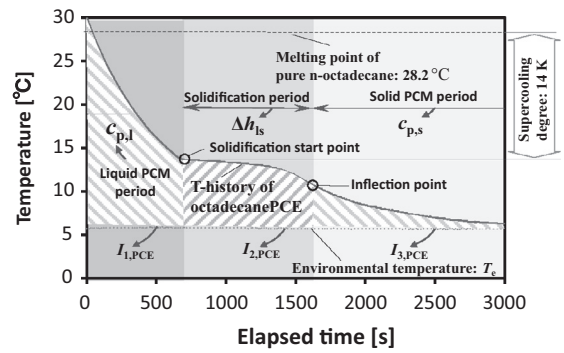


Fig. 8. Temperature history (PCM: 20.0 mass% n-octadecane).

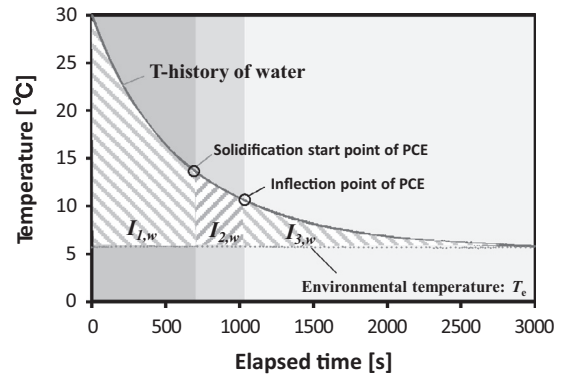


Fig. 9. Temperature history (reference: pure water).

$$c_{p,l} = \frac{m_{t,w}c_{p,t} + m_w c_{p,w}}{m_{PCE}} \frac{A_{t,PCE}}{A_{t,w}} \frac{I_{1,PCE}}{I_{1,w}} - \frac{m_{t,PCE}}{m_{PCE}} c_{p,t} \quad (7)$$

$$c_{p,s} = \frac{m_{t,w}c_{p,t} + m_w c_{p,w}}{m_{PCE}} \frac{A_{t,PCE}}{A_{t,w}} \frac{I_{3,PCE}}{I_{3,w}} - \frac{m_{t,PCE}}{m_{PCE}} c_{p,t} \quad (8)$$

$$\Delta h_{is} = - \left( \frac{m_{t,PCE}}{m_{PCE}} c_{p,t} + \frac{c_{p,l} + c_{p,s}}{2} \right) (T_m - T_i) + \frac{m_{t,w}c_{p,t} + m_w c_{p,w}}{m_{PCE}} \times \frac{A_{t,PCE}}{A_{t,w}} \frac{I_{2,PCE}}{I_{2,w}} (T_m - T_i) \quad (9)$$

where  $I_{1,PCE}$ ,  $I_{2,PCE}$  and  $I_{3,PCE}$  correspond to the area below the curve for the solid-phase, solidification and liquid phase periods, respectively. These areas are indicated by slashed areas in Fig. 8.  $I_{1,w}$ ,



**Table 2**  
Specific heat and latent heat of fusion of PCE (PCM: n-hexadecane).

Confidence interval [%]	$c_{p,l}$ [kJ/(kg K)]		$c_{p,s}$ [kJ/(kg K)]		$\Delta h_{sl}$ [kJ/kg]	
	2		2		6	
Mass fraction [mass%]	Experimental value	Estimation value	Experimental value	Estimation value	Experimental value	Estimation value
10.0	4.22 ± 0.19	3.97	4.12 ± 0.37	3.93	21.4 ± 1.7	22.9
16.7	4.07 ± 0.20	3.81	3.23 ± 0.14	3.74	38.7 ± 1.4	38.3
20.0	3.63 ± 0.19	3.73	2.73 ± 0.37	3.65	46.7 ± 1.6	45.9
25.0	3.47 ± 0.06	3.60	2.57 ± 0.31	3.48	58.5 ± 1.2	57.4

**Table 3**  
Specific heat and heat of fusion of PCE (PCM: n-octadecane).

Confidence interval [%]	$c_{p,l}$ [kJ/(kg K)]		$c_{p,s}$ [kJ/(kg K)]		$\Delta h_{sl}$ [kJ/kg]	
	2		2		6	
Mass fraction [mass%]	Experimental value	Estimation value	Experimental value	Estimation value	Experimental value	Estimation value
10.0	4.03 ± 0.11	3.97	3.97 ± 0.25	3.93	23.4 ± 1.2	24.4
16.7	3.93 ± 0.07	3.81	3.60 ± 0.10	3.74	38.1 ± 0.4	40.7
20.0	3.80 ± 0.31	3.73	3.57 ± 0.17	3.65	49.7 ± 0.6	48.7
25.0	3.67 ± 0.27	3.60	3.40 ± 0.40	3.48	61.1 ± 2.0	60.9

**Table 4**  
Flow condition of PCE.

	Pure water	n-Hexa-decane PCE	n-Octa-decane PCE	Remarks	
Tube diameter $D$ [m]	0.02			Common conditions for all fluids	
Amount of transported heat per second [W]	590				
Flow velocity $u$ [m/s]	0.05–0.09	0.02–0.06	0.02–0.06	Adjusted to set heat transported amount	
Reynolds number	1000–2000	20–1000	20–1000		
Range of temperature change during heat exchange [°C] (Temp. difference [K])	5 K 10 K	15.7–20.7 or 25.7–30.7 13.2–23.2 or 23.2–33.2	15.7–20.7 13.2–23.2	25.7–30.7 23.2–33.2	Calculation parameters

$I_{2,w}$  and  $I_{3,w}$  were obtained from the T-history of the reference material in Fig. 9.

To apply the T-history method, the lumped capacitance method [25] must also be applied to each test tube, because it simplifies the experimental system. To apply the lumped capacitance method, Eq. (10) must generally be satisfied:

$$Bi = \frac{\alpha R}{k} < 0.1 \quad (10)$$

The thermal conductivity of the PCE ( $k$ ) was calculated using the Maxwell-Eucken equation [26]:

$$k = k_{con} \frac{2(k_{con}/k_{PCM} + 1) + 2\phi(1 - k_{con}/k_{PCM})}{2(k_{con}/k_{PCM} + 1) - \phi(1 - k_{con}/k_{PCM})} \quad (11)$$

When the lumped capacitance method is applied, the bulk temperature of each sample can be regarded as uniform throughout the experiment. Therefore, the T-history during periods without phase change (i.e. the liquid and solid periods) can be expressed as:

$$T = (T_0 - T_e) \exp\left(\frac{\alpha A}{m c_p}\right) t + T_e \quad (12)$$

The heat transfer coefficient on the surface of the test tubes was calculated by applying Eq. (12) to the T-history response of the reference. The Biot number was calculated, and the range for PCEs containing 10.0–20.0 mass% of PCM was  $0.085 < Bi < 0.098$ . However, the Biot number of PCEs containing more than 25.0 mass% of PCM exceeded the applicable range for the lumped capacity method. Therefore, the result for the PCE containing 25.0 mass% of PCM is shown just for reference.

### 3.3.2. Experimental results and discussion

Thermophysical properties obtained from measurements of the PCEs are shown in Tables 2 and 3. Estimation values were calculated by regarding the PCE as a binary mixture of pure water and PCM. Specifically, the estimation values were obtained using thermophysical properties from the literature, and the content rates of pure water and the PCM.

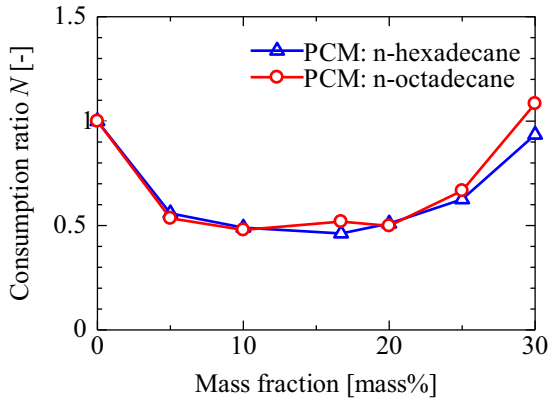
The 95% confidence interval was estimated to be within  $\pm 2\%$  at maximum for specific heat measurement, and to be within  $\pm 6\%$  for the latent heat measurement. It was considering the uncertainties of the primary (temperature and mass) measurements and literature values.

Tables 2 and 3 show that the latent heat measurements had a relatively small deviation of  $\pm 8\%$ . This was slightly larger than the interval estimated by uncertainty analysis. However, the specific heat results showed a large deviation from the estimation value, which might be due to characteristics of the T-history method. This method is sufficiently accurate to measure latent heat, but the accuracy of specific heat measurements depends on the type of PCM according to previous study [24]. It is likely that specific heat was not accurately measured in the present study, as well as the previous one.

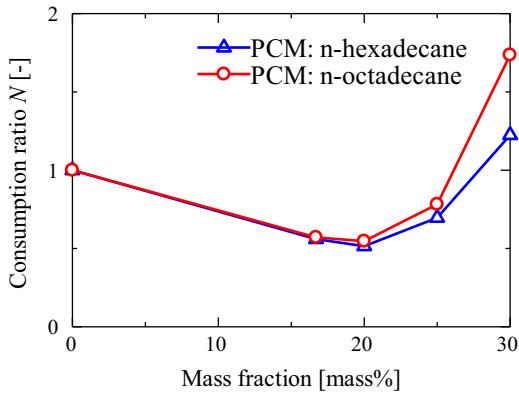
From the results, we conclude that if the thermal properties of the PCM are known, then the latent heat of the PCE can be predicted from its PCM mass fraction, even though the PCM is dispersed as fine particles.

## 4. Pumping power evaluation

The pumping power required to transport the PCEs were evaluated for their application as heat transport media. Evaluation was

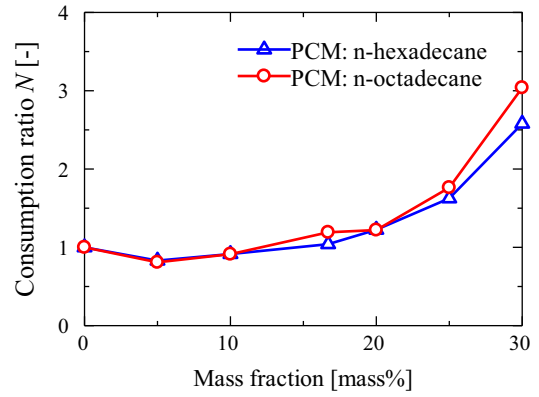


(a) PCM: Liquid-phase

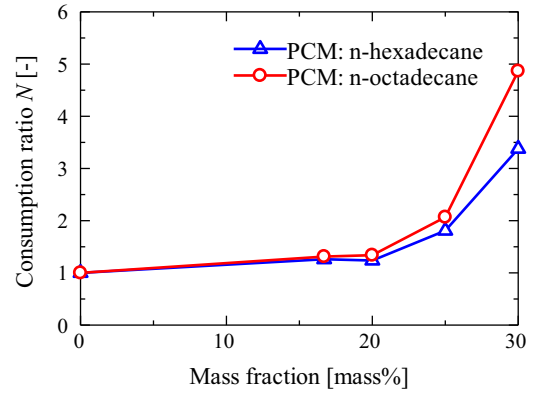


(b) PCM: Solid-phase

Fig. 10. Pump power estimation result (5 K difference).



(a) PCM: Liquid-phase



(b) PCM: Solid-phase

Fig. 11. Pump power estimation result (10 K difference).

based on the measured properties of the PCEs. Eqs. (13) and (14) were used to calculate the pumping power ( $P$ ) and pumping power ratio ( $N$ ) between pure water and the PCE:

$$P = 8L\mu\pi v^2 \quad (13)$$

$$N = \frac{P_{PCE}}{P_w} \quad (14)$$

The viscosity at 25.0 °C was used for that of the water and PCEs. The viscosity of PCEs measured in the present study is that of in the case of their dispersed phase are liquid PCM particles. Therefore, the viscosity of the PCE with solid PCM particles was calculated using Mooney’s equation in Eq. (4).  $\mu_{PCM}$  was regarded as infinite when the PCM particles are in the solid phase.

The flow conditions of the PCEs are shown in Table 4, and results of the calculations are shown in Figs. 10 and 11. The tube was assumed straight and insulated. The temperature ranges includes the melting point of each PCM. Assuming that the same amount of heat is transported by the same tube (diameter: 0.02 m) taking the same time, the following parameters were varied: (a) PCM type and mass fraction; (b) temperature difference between before and after heat exchange. The flow velocity was selected to the all fluids assumed to be in laminar flow region ( $Re < 2000$ ) and the heat transport amount per second of them were equalled.

The heat transportation pumping power ratios at temperature difference of 5 and 10 K indicated that the most efficient point shifted to lower mass fraction with increasing temperature difference. In the case of 5 K difference, the most efficient point exists within 10.0–20.0 mass%. However, in the case of 10 K difference, the most efficient point exists within 0–10.0 mass%. This was

because the heat transportation proportion of sensible heat increased with increasing temperature difference. Hence, the pump consumption increased because the viscosity effected stronger than the decrease in flow amount, which was caused by the increase in mass fraction and the most efficient point shifted to lower mass fraction.

### 5. Conclusion

PCEs containing n-hexadecane and n-octadecane PCMs were prepared, and their particle size distribution, viscosity, specific heat and latent heat were evaluated experimentally. The particle size distributions of all PCEs were similar, and independent of the dispersed phase mass fraction. The viscosity of the PCEs increased with increasing PCM mass fraction, and agreed well with Mooney’s equation, which is used to predict suspension viscosity. The PCE containing 40.0 mass% of PCM exhibited pseudoplastic behavior. The measured latent heats of the PCEs agreed with estimated values calculated assuming that the PCEs were simple mixtures of PCMs and pure water. Pump consumptions of the PCEs were calculated, and to be lower than that of water, because of the latent heat of PCMs.

### References

- [1] Fazilati M Ali, Alemrajabi A Akbar. Phase change material for enhancing solar water heater, an experimental approach. *Energy Convers Manage* 2013;71:138–45.
- [2] Biswas K, Abhari R. Low-cost phase change material as an energy storage medium in building envelopes: experimental and numerical analysis. *Energy Convers Manage* 2014;88:1020–31.

- [3] Chen J, Ling Z, Fang Xi, Zhang Z. Experimental and numerical investigation of form stable dodecane/hydrophobic fumed silica composite phase change materials for cold energy storage. *Energy Convers Manage* 2015;105:817–25.
- [4] Zhou G, Pang M. Experimental investigations on the performance of a collector-storage wall system using phase change materials. *Energy Convers Manage* 2015;105:178–88.
- [5] Chaiyat N. Energy and economic analysis of a building air-conditioner with a phase change material (PCM). *Energy Convers Manage* 2015;94:150–8.
- [6] Kouksou T, Jamil A, El Rhafiki T, Zeraouli Y. Prediction of the heat transfer coefficient for ice slurry flows in a horizontal pipe. *Energy Convers Manage* 2010;51:1311–8.
- [7] Kumano H, Hirata T, Shouji R, Shirakawa M. Experimental study on heat transfer characteristics of ice slurry. *Int J Refrig* 2010;33:1540–9.
- [8] Kumano H, Tamura F, Sawada S, Asaoka T. Study on flow and heat transfer characteristics of ice slurry in the transition region. *Int J Refrig* 2013;36:801–8.
- [9] Takahashi H, Kato M, Sasaki M, Kawashima T, Masuyama T. Pressure loss for ice-water slurry flows in pipelines. *J Multiph Flow* 1995;9(4):308–15.
- [10] Zhang P, Ma ZW. An overview of fundamental studies and applications of phase change material slurries to secondary loop refrigeration and air conditioning systems. *Renew Sustain Energy Rev* 2012;16:5021–58.
- [11] Zhang P, Ma ZW, Wang Z. An overview of phase change material slurries: MPCs and CHS. *Renew Sustain Energy Rev* 2010;14:598–614.
- [12] Inaba H, Morita S, Nozu S. Fundamental study of cold heat-storage system of O/W-type emulsion having cold latent-heat-dispersion material (1rd report). *Nippon Kikai Gakkai Ronbun Shu* 1993;59:282–9.
- [13] Chen B, Wang X, Zhang Y, Xu H, Yang R. Experimental research on laminar flow performance of phase change emulsion. *Appl Therm Eng* 2006;26:1238–45.
- [14] Huang L, Noeres P, Petermann M, Doetsch C. Experimental study on heat capacity of paraffin/water phase change emulsion. *Energy Convers Manage* 2010;51:1264–9.
- [15] Fumoto K, Kawazi M, Kawanami T. Characteristics of nano-emulsion for cold thermal storage – 1st report: stability and viscosity. *Trans JSRAE* 2009;26(3):265–71.
- [16] Delgado M, Lazaro A, Mazo J, Penalosa Conchita, Dolado Pablo, Zalba Belen. Experimental analysis of a low cost phase change material emulsion for its use as thermal storage system. *Energy Convers Manage* 2015;106:201–12.
- [17] Sagitani H, Hattori T, Nabeta K, Nagai M. Formation of O/W emulsion having fine and uniform droplets by the surfactant (D) phase emulsification method. *Nippon Kagaku Kaishi* 1983;10:1399–404.
- [18] Kumashiro J, Togashi K, Kawanami T, Fumoto K, Hirano S. Thermal characteristics of emulsion containing nano size phase change particles. In: *Proceedings of the 10th Asian thermophysical properties conference*; 2013.
- [19] Nobuhiro S. *Tikunetsu kogaku*. Morikita Shuppan 1995.
- [20] Thomas DG. Transport characteristics of suspension: Viii a note on the viscosity of Newtonian suspensions of uniform spherical particles. *J Colloid Sci* 1965;20:267–77.
- [21] Mooney M. The viscosity of a concentrated suspension of spherical particles. *J Colloid Sci* 1951;6:162–70.
- [22] Matsumoto S. The viscosity of emulsions. *Nippon Rheol Gakkaishi* 1989;17:110–5.
- [23] Hong H, Kim SK, Kim Y. Accuracy improvement of T-history method for measuring heat of fusion of various materials. *Int J Refrig* 2004;27:360–6.
- [24] Kouksou T, Rhafiki TE, Mahdaoui M, Bruel P, Zeraouli Y. Crystallization of supercooled PCMs inside emulsions: DSC applications. *Sol Energy Mater Sol Cells* 2012;107:28–36.
- [25] Holman JP. *Heat transfer*. 10th ed. New York: McGraw-Hill Science; 2009. p. 141–3.
- [26] Hayashi K, Saijo Y, Uei I. On the expression for thermal conductivity of two-phase media. *Yogyo-Kyokai-Shi* 1974;82(6):318–24.